A Molecular Model for Muscle Contraction

K. C. HOLMES

Max Planck Institut für medizinische Forschung, Jahnstrasse 29, 69120 Heidelberg, Germany.
E-mail: holmes@otto.mpimf-heidelberg.mpg.de

Abstract

The molecular mechanism of muscle contraction has been elucidated by a combination of electron microscopy, biochemistry and X-ray diffraction from fibres and crystals. Protein crystallography provided the essential molecular anatomy for understanding this problem. Synchrotron radiation has played a crucial role.

1. Introduction

Modern muscle research starts with the publication of the sliding filament hypothesis (Huxley & Niedergerke, 1954; Huxley & Hanson, 1954), which proposed that the contraction of muscles took place by the mutual sliding of two sets of filaments: thick and thin (Fig. 1). These early studies were base on light-microscopic investigations. At the same time, H. E. Huxley developed ultra-thin sectioning to examine single layers (*ca* 200 Å thick) of filaments by electron microscopy. He was able to show that the thick filaments contain the protein myosin and the thin filaments the protein actin. Moreover, he was able to visualize the 'cross-bridges', a part of the myosin molecule that extends out from the thick filaments and interacts with the thin filaments (Huxley, 1957). X-ray fibre diffraction from insect flight muscles showed that the cross-bridges took two distinct orientations in the presence and absence of ATP (adenosine triphosphate). These two states were characterized by electron microscopy (Reedy *et al.*, 1965) and became known as the 45 and 90° orientations.

After studying at Cambridge, UK, K. C. Holmes carried out his doctoral research at Birkbeck College London under the supervision of Rosalind Franklin on the structure of tobacco mosaic virus. After a sojourn in Boston, he returned to Cambridge to the newly open MRC Laboratory of Molecular Biology. In 1968, he moved to Heidelberg to open a new Department of Biophysics at the Max Planck Institute of Medical Research. He pioneered the use of synchrotron radiation as an X-ray source for diffraction experiments. His laboratory solved the structure of actin and the actin filament.

The relative sliding of thick (myosin) and thin (actin) filaments is brought about by the cross-bridges which interact cyclically with the actin filaments, transporting them by a kind of rowing action (Huxley, 1969). The movement is powered by the hydrolysis of ATP (Fig. 2). In the absence of ATP, myosin binds tightly to actin. This association is often referred to as the 'rigor complex' since it occurs in muscle shortly after death when all ATP stores are depleted. However, on binding to the ATPase site on the myosin cross-bridge, ATP rapidly dissociates the actomyosin complex; ATP is hydrolysed and forms a stable myosin-products complex (adenosine diphosphate + phosphate, ADP·P_i); actin recombines weakly with this complex. After recombining with actin, the cross-bridge undergoes a conformational change leading to the rowing-like stroke (sometimes referred to as the power stroke) which translates the thin filament past the thick filament (there are thousands of cross-bridges on a thick filament that bring about this motion in concert). During this process, the products of hydrolysis are released (Lymn & Taylor, 1971) and the actin–myosin returns to the strong rigor complex.

This model is known as the *swinging cross-bridge model* for muscle contraction. Originally, it was thought that the cross-bridge would swing about a pivot point at the actin myosin interface. Over the years, this became less and less likely (Cooke, 1986) and in the light of recent results the swinging cross-bridge has been amended into a *swinging lever arm* (Fig. 3), in which the bulk of the cross-bridge is envisaged to bind to actin with a more or less fixed geometry and only the distal (C-terminal) part of the myosin molecule moves (Holmes, 1997).

1.1. *Low-angle X-ray fibre diagrams*

Muscle fibres give detailed low-angle X-ray fibre diagrams which arise from the hexagonal arrangement of the thick and thin filaments (Huxley, 1952). Along the meridian of the fibre diagram is a series of reflections arising from the regular array of myosin cross-bridges along the thick filament. Variations of the strength of these reflections have been shown to be correlated with the movement of the cross-bridges (Reedy *et al.*, 1965). X-ray fibre diffraction patterns can be obtained from functional excised frog muscles, therefore changes in the

diffraction pattern can be observed during a contraction (Huxley & Brown, 1967). However, to extend such observations into the time domain requires much stronger X-ray sources than could be provided by even the best rotating-anode X-ray tubes. This requirement drove the pioneering use of synchrotron radiation as a source for X-ray diffraction (Rosenbaum *et al.*, 1971). Subsequently, synchrotron radiation enabled the study of contracting frog muscle with ms time resolution (Huxley *et al.*, 1981) and later with a resolution of 200 ms (Irving *et al.*, 1992).

Such experiments provided evidence that cross-bridges do in fact move during a contraction.

2. Structures of actin and myosin

2.1. *Atomic structure of actin*

Thin filaments (*F*-actin) are helical polymers that have 13 actin molecules (42 kDa) arranged on 6 left-handed turns repeating every 360 Å. The rise per subunit is 27.5 Å. The morphology of the actin helix is two intertwined long-pitch right-handed helices. Along each of the morphological helices, the actin monomers

are spaced by 55 Å. The structure of the monomer (*G*-actin) was solved by protein crystallography as a complex with DNAase I (Kabsch *et al.*, 1990) (Fig. 4). The structure shows actin to consist of two similar domains each of which contains a five-stranded β-sheet and associated α-helices. The phosphate moiety of a nucleotide (ATP or ADP) is bound between the two β-sheet domains. Each of the domains carries a sub-domain: one is involved in actin–actin interactions and the other forms the top of the nucleotide-binding pocket. Somewhat unexpectedly, the structure showed actin to belong to a family of kinases and ATPases that includes hexokinase and the heat-shock protein HSC70 (see Kabsch & Holmes, 1995).

Orientated gels of filamentous actin yield X-ray fibre diagrams to about 6 Å resolution. Fibre diffraction patterns were calculated from models produced by placing the *G*-actin atomic structure in the helix for all possible orientations. A computer search compared the calculated and observed X-ray fibre diagrams to find the best fit (Holmes *et al.*, 1990). The solution was then
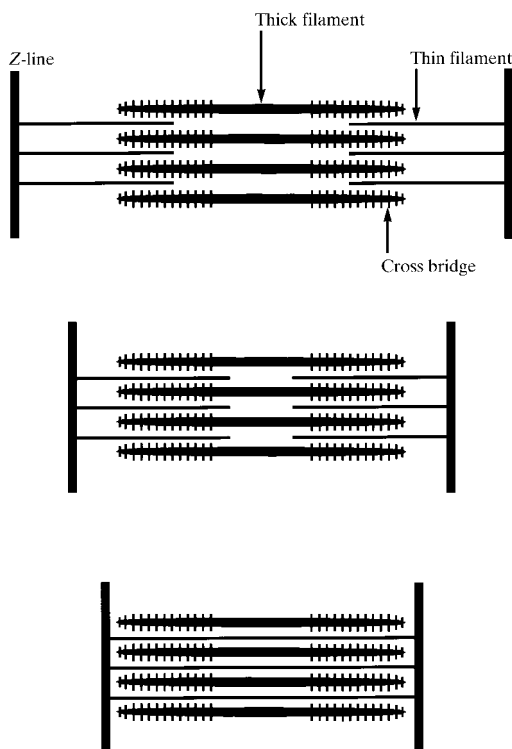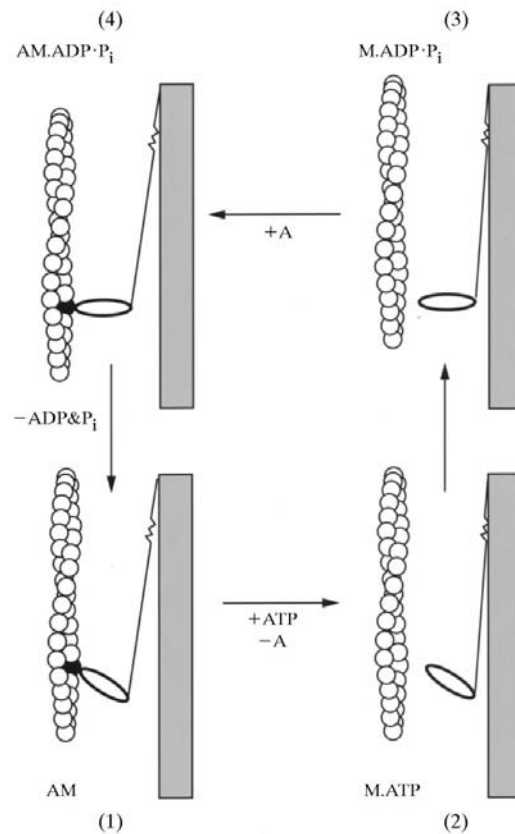

Fig. 1. During muscle contraction, two sets of interdigitating filaments, the 'thick' (myosin) filaments and 'thin' (actin) filaments slide past each other to produce a shortening of each sarcomere, the unit of muscle structure. The relative movements of the two types of filament are brought about by the 'myosin cross-bridges' which protrude from the thick filaments and interact cyclically with the thin filaments.

Fig. 2. The Lymn–Taylor cycle (Lymn & Taylor, 1971): the myosin cross-bridge is bound to actin in rigor 45° position ('down') (1). ATP binds, which leads to very fast dissociation from actin (2). The hydrolysis of ATP to ADP and P_i leads to a return of the myosin cross-bridge to the 90° 'up' position, whereupon it rebinds to actin (3). This leads to release of the products and return to (1). In the last step, actin is 'rowed' past myosin.

refined to allow for the conformational changes taking place in actin on polymerization (Lorenz *et al.*, 1993) (Fig. 5). The most notable movement is that the subdomains move 3–4 Å closer together in *F*-actin closing off the ADP binding site, which leads to a very low nucleotide exchange rate (the nucleotide in *F*-actin plays a structural rather than a metabolic role). The contacts along the two long-pitch helices are substantial in area (> 3000 Å^2) in accord with the fact that the total pull on the filament (∼1000 pN) is transmitted through this contact.

2.2. *Atomic structure of myosin*

The myosin molecule consists of six polypeptide chains, two 'heavy chains' and four 'light chains'. Most of the length of the heavy polypeptide chains is involved in a dimer that consists of a long α-helical coiled coil. The N-terminal parts of each heavy chain leave the coiled coil to form the cross-bridges, whereas the α-helical coiled coils assemble to form the thick filaments. The cross-bridges point out from the surface of the thick filament. Controlled proteolysis allows the cross-bridge to be cleaved away from the rest of the myosin molecule. This fragment (120 kDa, referred to as S1) contains all the enzymatic activity of myosin and contains two light chains in addition to the heavy chain (Margossian & Lowey, 1973a,b). Further limited proteolysis breaks S1 into three fragments named after their apparent molecular weights – 25K (N-terminal), 50K (middle), and 20K (C-terminal) (Mornet *et al.*, 1979). These fragments were thought to represent subdomains of S1. The structure of S1 (see below) shows them rather to mark the positions of flexible loops in S1.

The first X-ray crystal structure of a myosin fragment was of S1 from chicken muscle without bound nucleotide (Rayment, Rypniewski *et al.*, 1993). The structure shows the S1 to be tadpole-like in form (Fig. 6), with an elongated head consisting of a seven-stranded β-sheet and a C-terminal tail. All three fragments (25K, 50K and 20K) contribute to the seven-stranded β-sheet. Numerous α-helices that surround the β-sheet form a deep cleft extending to the actin binding site. The C-terminal tail, which in the intact myosin molecule is connected to the thick filament, forms an extended α-helix, which binds the two calmodulin-like 'light chains'.

In the following description, we refer to the chicken skeletal myosin sequence because of its biochemical familiarity although most subsequent work has actually
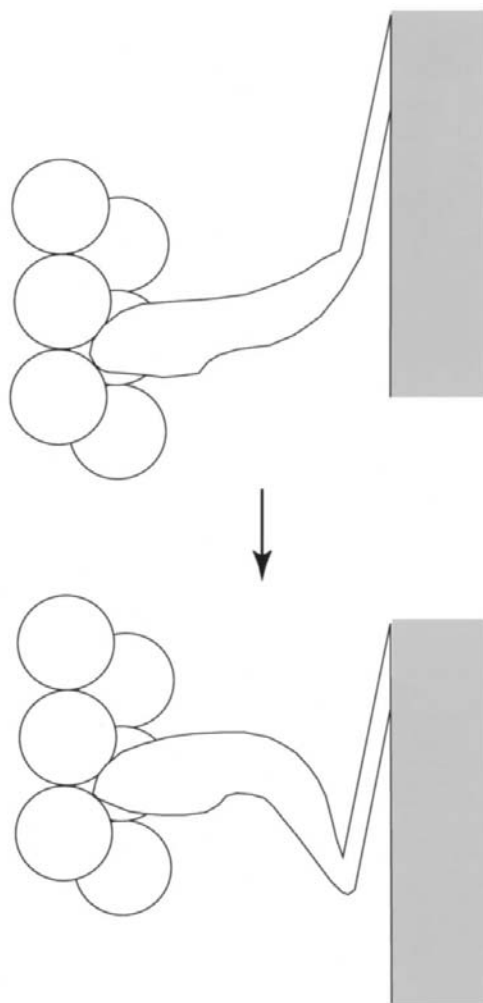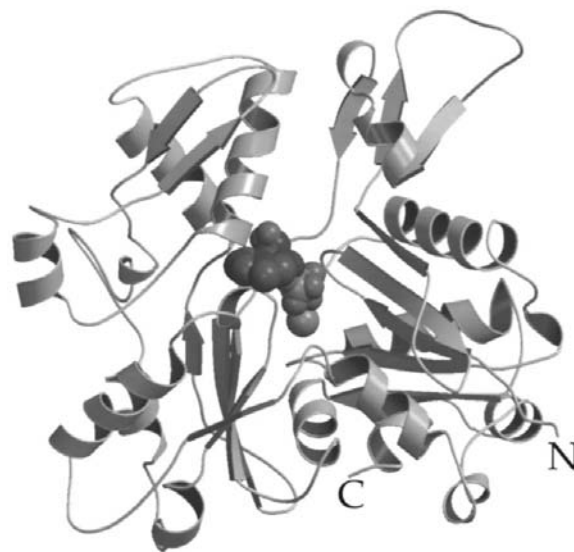

Fig. 3. Numerous experiments indicated that the scheme shown in Fig. 2 needed revision: only the distal part of the cross-bridge moves (Cooke, 1986).

Fig. 4. Structure of the actin monomer (Kabsch *et al.*, 1990). This consists of two α–β domains with ADP bound between them. The ADP complexes a Ca^{2+} ion. Each domain can be subdivided into two subdomains. The polypeptide chain crosses twice between the domains so that both the N- and C-terminii are in the right-hand domain. Figure prepared with *MOLSCRIPT* (Kraulis, 1991) and *raster3D* (Merritt & Bacon, 1997).

been carried out on *Dictyostelium* (cellular slime mold) myosin. Following Rayment *et al.*, the proteolytic fragments are colour coded: 25K (N-terminal) green; 50K red; and 20K (C-terminal) blue (Fig. 6). The 50K fragment actually spans two domains which Rayment *et al.* have called the 50K upper domain and the 50K lower domain or actin binding domain. In subsequent pictures, the actin binding domain has been coloured white. The N-terminus lies near the tail and the first 80 residues form a protruding SH3(thiol)-like β-barrel domain of unknown function [not present in all myosins (Cope *et al.*, 1996)]. The rest of the 25K fragment and the 50K upper fragment together (81–486) form one domain which accounts for six of the seven strands of the β-sheet that constitutes the bulk of the molecule. The ATP binding site is in this large domain near the 25K–50K fragment boundary and contains a characteristic *P* loop similar to that found in some other ATPases and *G*-proteins. The ATP binding site is about 40 Å from the actin binding site. The 50K lower fragment (487–600) actually forms a well defined domain that constitutes the major part of the actin binding site. A large positively charged disordered loop (625–647) follows which is also involved in actin binding. The first part of the ensuing 20K domain (648–689) is an integral part of the 25K–

50K domain and consists of a long helix running from the actin binding site to a seventh strand of the β-sheet. This is followed by a turn and a broken helix containing two reactive thiols (SH1 707 and SH2 697). The SH1 helix possibly forms part of the hinge for the ensuing lever. There follows a small compact domain (711–781) which has been termed the 'converter domain'

Fig. 6. (*a*) Structure of myosin S1 (Rayment, Rypniewski *et al.*, 1993). The molecule has three polypeptide chains, one 'heavy' and two 'light'. The heavy chain forms a large globular domain based on a seven-stranded β-sheet which contains the ATP binding site and the actin binding. A long C-terminal α-helical 'neck' or 'tail' is attached. The light chains bind to the neck. For details see text. (*b*) The myosin motor domain in an orientation similar to that shown in the following actin–myosin complexes. Note the two 'loops' (which are unstructured) can be cleaved by trypsin to yield the 25K N-terminal fragment (green), the 50K middle fragment (red and white) and the 20K C-terminal fragment (blue). The 50K fragment can be subdivided into two subdomains. Together with the 25K fragment and one strand from the 20K fragment, the N-terminal part (red) forms a seven-stranded β-sheet. This β-sheet carries a *P*-loop which forms an important part of the nucleotide binding site. The C-terminal domain of the 50K fragment (called the 50K lower domain) or actin binding domain) (white) is conserved and is an important component of the actin binding site. Figures prepared with *MOLSCRIPT* (Kraulis, 1991) and *raster3D* (Merritt & Bacon, 1997).

Fig. 5. Structure of the actin helix (*a*) before refinement (Holmes *et al.*, 1990), (*b*) after refinement (Lorenz *et al.*, 1993). Figures prepared with *GRASP* (Nicholls *et al.*, 1991).
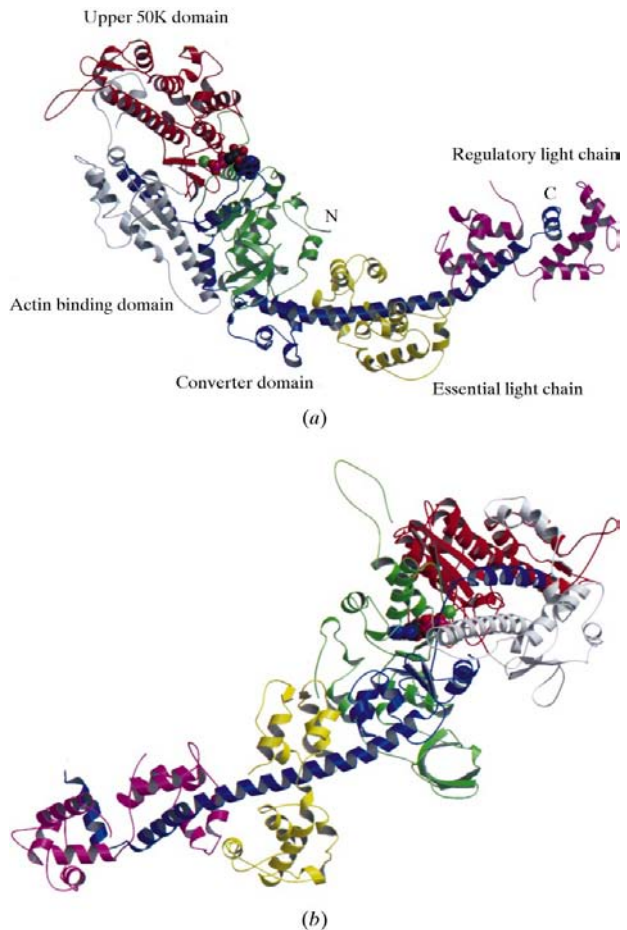
(Houdusse & Cohen, 1996). This apparently functions as a socket for the C-terminal α-helical tail that carries the two light chains which has been called the 'regulatory domain' or 'neck'. The main function of the regulatory domain or neck, however, appears to be as a 'lever arm' to amplify rotational movements experienced by the converter domain during ATP hydrolysis.

2.3. Actomyosin

An atomic model of the actin–myosin complex (Rayment, Holden et al., 1993; Schroeder et al., 1993) was obtained by fitting the atomic structures of F-actin and S1 into three-dimensional cryoelectron microscope reconstructions of 'decorated actin' (Fig. 7). Decorated actin is produced by incubating F-actin with S1 in the absence of nucleotides. One cross-bridge (S1) binds to each actin monomer. Decorated actin is taken as a model of the rigour complex between actin and myosin. The atomic model of chicken muscle S1 was without nucleotide and therefore is thought to be in the rigor configuration. S1 binds to the lower side of one domain of actin but with a considerable contact to the sub-domain of the next actin molecule below. The actin binding sites and nucleotide binding sites are on opposite sides of the sheet and are separated by about 40 Å. The cleft in myosin extends from the ATP binding site to the actin binding site so that movements in this cleft co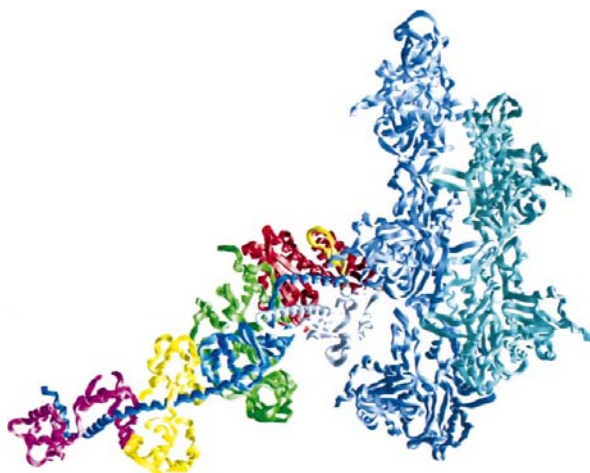uld provide the physical link between the ATP site and the actin binding site. Furthermore, the very extended C-terminal α-helix of S1 lies distal to the actin helix and is ideally placed to be a putative lever arm.

3. The swinging lever arm

3.1. Electron microscopy

One might expect myosin S1 to be at the top of the power stroke in the presence of the products of hydrolysis of ATP (Fig. 2). A suitable system for observing such a conformational change is 'decorated actin' which gives us a reference structure for the end of the power stroke. Unfortunately, corresponding data in the presence of ATP are difficult to get because the proteins dissociate rapidly on adding ATP. Therefore, Milligan, Sweeney and co-workers investigated the effects of adding ADP, which, although it does not produce such a large reduction in actin–myosin affinity, in suitable muscles would be expected to lead to a partial reversal of the power stroke. Cryoelectron micrograph reconstructions of actin decorated with smooth-muscle

Fig. 7. The structure of the actin–myosin complex (Rayment, Holden et al, 1993; Schroeder et al., 1993). Shown are (right) five actin molecules in an actin helix and (left) a myosin cross-bridge (S1). Shown are: the 25K fragment (green); the 50K upper fragment (red); the 50K lower fragment (white); the disordered chain between the 50K domain and the 20K domain is shown as a yellow loop – note that this loop has been modelled; the first part of the 20K domain including the SH2 helix (until 699) is shown as light blue; the SH1 helix, converter domain and the C-terminal helix – 'the neck' – as dark blue; the regulatory light chain as magenta; and the essential light chain as yellow. Figure prepared with GRASP (Nicholls et al., 1991).
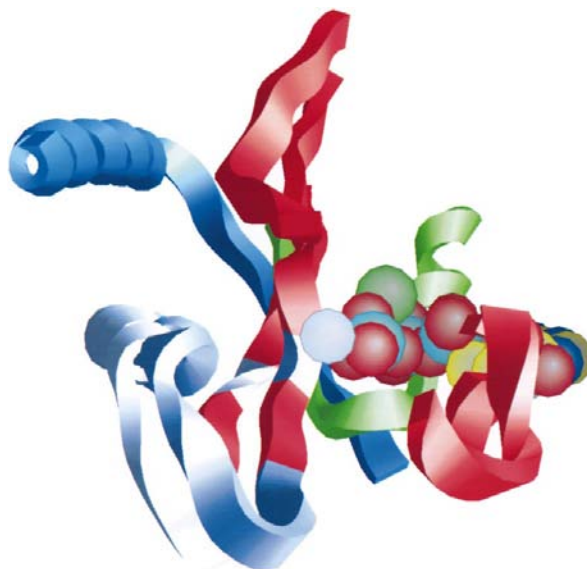

Fig. 8. A view of the ATP binding site looking out from the actin helix. Shown are: the P-loop (green); an MgATP molecule with the base at the back and the three phosphate groups in the front (carbon yellow, nitrogen blue, phosphate light blue, oxygen red, magnesium green); the position of a putative attacking water for the hydrolysis is also indicated (white); parts of the 50K upper domain (red) including the so called 'switch-1' region (right); the switch-2 region which is at the upper-50K/actin-binding-domain boundary, in the open 'ADP' (light grey) and closed 'ATP' (blue-grey) conformations – the position of the conserved glycine (466) is indicated in white (note that this residue moves about 5 Å between the two conformations); the helix (648–666) acts as fulcrum for the relative rotation of the 50K upper and lower domains (blue). Coordinates taken from Fisher et al. (1995), Schlichting et al. (1998) and Smith & Rayment (1996a). Figure prepared with GRASP (Nicholls et al., 1991)

myosin by Milligan *et al.* do show a 30–35° rotation of the lever arm away from rigor on binding ADP (Jontes *et al.*, 1995; Whittaker *et al.*, 1995). This experiment provided the first direct demonstration of the anticipated lever-arm swing.

3.2. *What happens if you make the lever longer?*

Spudich and collaborators (Uyeda *et al.*, 1996) were able to alter the length of the neck in *Dictyostelium discoideum* (cellular slime mold) myosin II S1 (which is homologous to vertebrate skeletal myosin) by adding or subtracting light-chain binding regions. An *in vitro* motility measurement of the speed of transport of actin filaments across a lawn of S1 molecules irrigated with ATP showed a velocity of actin transport that was proportional to the length of the lever arm. Furthermore, the intercept of the graph at zero velocity corresponds to the position of the SH1-containing helix, again indicating the possible function of this region as a putative hinge.

In a similar experiment, Manstein and his collaborators (Anson *et al.*, 1996) have replaced the neck region with artificial lever arms consisting of one or more α-actinin repeats (a triple α-helix motive) and have used the engineered myosin *in vitro* motility assays. As above, the authors find the speed of transport is proportional to the length of the lever arm. Kinetic measurements showed that the variation in speed of transport of actin could not be accounted for by alterations in the ATPase activities since these were essentially unaffected by the presence or number of α-actinin repeats (Kurzawa *et al.*, 1997). Therefore, they conclude that the length of the lever arm controls the velocity of transport.

3.3. *Fluorescent markers*

Specific fluorescent markers on the 'regulatory' light chain show a small angular movement on contraction (Irving *et al.*, 1995), whereas the 'lever-arm hypothesis' expects about 60° rotation However, if only a fraction (*ca* 10%) of the cross-bridges in active muscle take part in contraction at any one time, the magnitude of this apparent rotation can be proportionally scaled up towards the anticipated value.

All these experiments are consistent with a rotating lever arm with a hinge near the SH1 (707). Moreover, chemical cross-linking studies on the reactive thiol groups SH1 and SH2 point to this region as being sensitive to the presence and state of the nucleotide (Huston *et al.*, 1988) and possibly to be close to the putative 'motor'.

4. Crystallographic studies show myosin has two conformations

The myosin cross-bridge would be expected to have two discernible conformations: (i) when it first attaches to actin with the products of hydrolysis still bound with the lever at the beginning of the 'power stroke'; and (ii) at the end of the 'power stroke' when the phosphate and ADP are released (rigor). The end state is also called 'strong' because it binds to actin tightly, whereas the initial state is called 'weak' because of its low affinity for actin (see Geeves & Conibear, 1995). We might anticipate that these two states of the myosin cross-bridge might exist independently from actin and indeed protein crystallography shows this to be the case.

4.1. *Dictyostelium myosin*

Genetic manipulation of myosin is restricted to expression in eukaryotic hosts since myosin cannot be successfully expressed in prokaryotes. Rayment and his group have studied a crystalline fragment of *Dictyostelium* myosin II S1 expressed in the slime mold *Dictyostelium discoideum* which has been truncated after residue 781 (761 in *Dictyostelium* myosin). The truncation eliminates the neck and the associated light chains but the converter domain is still present. The expressed fragment corresponds with the myosin 'core' which has been identified by sequence comparisons to be common to all myosins – many myosins have quite different necks to skeletal muscle myosin but all have very similar 'cores' (Cope *et al.*, 1996). Experiments with shorter constructs show that damage to the converter domain leads to S1 constructs with bizarre ATPases. However, the form truncated at 781 appears kinetically normal (C. Bagshaw, personal communication).

4.2. *Myosin has two conformations*

The crystal structures of the truncated *Dictyostelium* myosin have been determined with a number of ATP analogues, particularly $ADP \cdot BeF_x$, $ADP \cdot AlF_4$ (Fisher *et al.*, 1995) and ADP·vanadate (Smith & Rayment, 1996a). (ADP·vanadate complexes are used as analogues of the transition state or possibly of the $ADP \cdot P_i$ state). While the $ADP \cdot BeF_x$ state looks similar to chicken muscle without nucleotide, the ADP·vanadate structure shows dramatic changes in shape of the S1 structure. These changes are also apparent with $ADP \cdot AlF_4$. There is a partial closing of the 50K upper/lower domain cleft, particularly around the γ-phosphate binding pocket, and large movements in the C-terminal region. The 50K upper and lower domains rotate a few degrees with respect to each other around the helix 648–666 in a way that closes the nucleotide binding pocket (Fig. 8) – a movement of some 5 Å. At the same time, the outer end of the long helix (the so-called switch-2 helix, residues 475–507) bends out by 24° at residue 497. This causes a rotation of the converter domain (711–781) to which the switch-2 helix is tightly linked by 70°. The fulcrum is provided by the mutual rotation of the
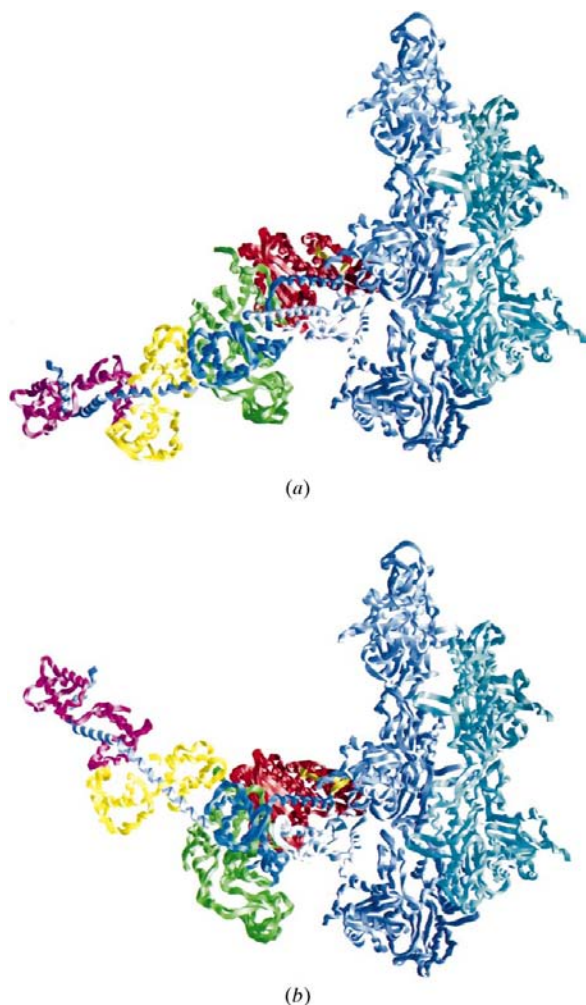
Fig. 9. (a) The 'end' state: the rigor complex (as in Fig. 7) modelled from the crystallographic data on the *Dictyostelium* myosin motor domain truncated at residue 781 (*Dictyostelium* 761) and complexed with ADP·BeF$_x$ (Fisher *et al.*, 1995). To establish the orientation with respect to the actin helix (right), the 50K upper and lower domains have been superimposed on the corresponding domains in the rigor structure shown in Fig. 7. The missing 'neck' region or lever arm (light blue) has been modelled from the chicken S1 data (Rayment, Rypniewski *et al.*, 1993) by superimposing the converter domains. Although the motor domain has bound nucleotide, it appears to be close to the rigor state. (b) A reconstruction of the 'beginning' state from the crystallographic data on the *Dictyostelium* construct truncated at 761 and complexed with ADP·vanadate (Smith & Rayment, 1996a) complemented with data from Schlichting *et al.* (1998). The state is postulated to be the state typical of ATP tight binding or of the products complex. The nucleotide binding site is closed. Note the 70° rotation of the converter domain. The missing 'neck' or lever arm has been modelled from chicken S1 data (Rayment, Rypniewski *et al.*, 1993) by superimposing the converter domains. The rotation of the converter domain is controlled by the bending out of the 'switch-2' helix which is adjacent to the switch-2 region. The end of the lever arm moves about 120 Å between the two states. Figures prepared with *GRASP* (Nicholls *et al.*, 1991).

distal part of the SH1–SH2 helix around the distal part of the switch-2 helix.

A model of this new state is shown in Fig. 9(b). The coordinates of the missing lever arm have been generated from the chicken myosin coordinates by superimposing the converter domains. For comparison, in Fig. 9(a) we show the corresponding diagram from the coordinates with ADP·BeF$_x$ bound in the active site (Fisher *et al.*, 1995) which, for reasons stated below, we take to be the ADP state (*i.e.* the state after release of the γ-phosphate). The end of the lever arm has moved through 120 Å along the actin helix axis.

4.3. *Switch-2 should close to enable ATP hydrolysis*

Smith & Rayment (1996b) note the similarity of the active site of myosin in the closed form with ras p21 and other *G*-proteins. The differences between the open and closed forms of the myosin cross-bridge in the neighbourhood of the active site reside almost entirely in the conformation of the linker region (465–470), which joins the 50K upper and lower domains. Smith & Rayment point out that this region is structurally equivalent to the switch-2 region in ras p21 with which it also has a very strong sequence homology. The mutual rotation and closing of the 50K upper/lower domains cleft causes this region to move by about 5 Å. In the chicken crystal structure (open form), which has no bound nucleotide and should therefore be close to the rigor conformation, the switch-2 region is not part of the nucleotide binding pocket. The same is true for the Fisher *et al.* ADP·BeF$_x$ structure. A similar movement of the switch-2 region depending on whether di- or trinucleotide is bound is also found in the *G*-proteins. Only in the closed form (ADP·vanadate) can the hydrogen bond between the carbonyl of G466 and the γ-phosphate (Fig. 8), which is an invariant characteristic of the *G*-protein active sites, be formed. Because of the importance of G466 (and neighbouring residues particularly the salt bridge R245–E468) for hydrolysis, it is difficult to see how hydrolysis can proceed in the open (rigor) form which would therefore appear not to be an MgATPase: the closing would appear to be essential for hydrolysis.

4.4. *ADP·BeF$_x$ can produce both open and closed states*

ADP·BeF$_x$ is thought to be an analogue for ATP. Fisher *et al.* (1995) solved the structure of truncated *Dictyostelium* S1 with ADP·BeF$_x$ bound in the active site and found it to be remarkably similar to chicken S1 without nucleotide. This result appears to show that the structure of the ATP state is 'open', which is puzzling since it would not be able to hydrolyse the ATP. Moreover, the attitude of the converter domain (and hence the 'neck') is close to rigor, which is also unexpected for the ATP state. One way out of this dilemma is to assume that this crystal form is not actually the ATP form but rather an ADP form. These comments apply

also to the other crystal forms of *Dictyostelium* S1 with other ATP analogues that show the 'open' structure (Gulick *et al.*, 1997). Since they have the same structure as the ADP form, they are apparently in this respect ADP analogues rather than ATP analogues. Recently, Schlichting *et al.* (1998) have solved the structure of an ADP·BeF$_x$ complex of truncated S1 and find it to be essentially identical to the ADP·vanadate complex. The active site is closed and the converter domain is in the rotated configuration. The construct used in this case was seven residues shorter than that used by Fisher *et al.* This results in a tighter binding of ADP (Kurzawa *et al.*, 1997). Apparently, in the shorter construct, the binding energy of ADP·BeF$_x$ is adequate to tip the scales for the closed ATP-like structure, whereas in the longer construct it was not. Therefore, one can picture the transition between the two forms of myosin as being sensitively poised: the structure solved by Fisher *et al.* apparently corresponds to the ADP-bound state whereas the structure solved by Schlichting *et al.* corresponds to the ATP-bound (or products complex) state.

It is in fact not yet clear which factors determine the structural preferences of the myosin S1. At present, it is simplest to classify on the basis of structure, *i.e.* is the lever arm up or down and is the ATP binding site closed or open?

4.5. γ-Phosphate release

Actin probably binds to the open form of the 50K upper/lower cleft and thereby facilitates phosphate release. The closed structure found with the ADP·vanadate generates a tight hydrogen-bonding pattern for the γ-phosphate, which probably explains the high phosphate affinity. This interaction in turn is important for stabilizing the closed form. Opening the cleft destroys the γ-phosphate binding pocket. Energy-filtered cryoelectron microscopy of decorated actin (Schroeder *et al.*, 1998) shows that the cleft may be open in the actin–myosin complex. Therefore, it seems likely that actin binding opens the cleft rather than closes the cleft as was suggested earlier. It seems that opening the cleft destroys the phosphate binding site and facilitates γ-phosphate release [a 'back door enzyme' (Yount *et al.*, 1995)].

4.6. *There are more states to come*

Although kinetic studies provide evidence that the actin–myosin binding in the presence of nucleotide is a multistep process, we do not yet have structural data on an initial weak binding of the closed form to actin. However, a consistent scheme may be developed by postulating that there is an additional transitory state, a bent closed form. We suppose that actin binds myosin with one main set of contacts at approximately

constant geometry, namely as is seen in the rigor actin–myosin complex (*i.e.* the open form of myosin). The 50K lower domain probably forms the invariant contacts to actin: the switch from weak to strong binding probably involves the recruitment of loops (the 50K–20K loop and the '404' loop) from the 50K upper domain to form the strong binding state. When confronted with myosin in the closed form, actin probably binds the 50K lower domain first, which binds actin weakly. An induced conformational change produces the open form which releases the γ-phosphate and binds actin strongly. Further changes associated with the release of ADP have yet to show up crystallographically. Moreover, it is not yet clear how nucleotide binding controls actin affinity. The changes in the actin binding region we presently observe seem rather small. Therefore, we eagerly await further crystal structures which may allow us more insight into myosin's rich polymorphism.

5. Summary

At present, crystallographic studies show two distinct structural states for myosin S1: the 'open' or 'end' conformation which is characterized by the absence of γ-phosphate and is close to rigor; and the 'closed' or 'beginning' state, which is favoured by binding ATP or the products complex (ADP·P$_i$). As a framework for understanding contraction, we propose that myosin transports actin by switching between these two states. 'Open' and 'closed' refer to the status of the ATP binding site. This in turn is coupled to the rotation of a C-terminal lever arm. In the 'closed' form, the lever arm is at the beginning of the power stroke whereas in the 'open' form it is at the end of the power stoke. The preference for 'open' or 'closed' is also controlled by binding to actin. We hypothesize that the closed state binds only weakly to actin. On this basis, we can correlate the structural states with the Lymn–Taylor cycle (Fig. 2).

Starting from an actin–myosin complex at the end of the power stroke, the binding of ATP brings about rapid closure of the cleft and concomitant release from actin. The closed state hydrolyses ATP to ADP·P$_i$ without attaching to actin. Thereafter, the rebinding of myosin in the closed or 'beginning' conformation of the products complex to actin opens the cleft to facilitate release of the γ-phosphate. Release of phosphate induces an isomerization to the open 'end' conformation since it is the presence of the γ-phosphate that stabilizes the closed form. The isomerization results in large changes of angle of the 'lever arm' (at the distal part of the myosin head). Since the S1 is strongly attached to actin at this stage, this results in a 120 Å transport of actin past myosin.

References

Anson, M., Geeves, M. A., Kurzawa, S. E. & Manstein, D. (1996). *EMBO J.* **15**, 6069–6074.

Cooke, R. (1986). *CRC Crit Rev. Biochem.* **21**, 53–118.

Cope, T. V., Whisstock, J., Rayment, I. & Kendrick-Jones, J. (1996). *Structure*, **4**, 969–987.

Fisher, A. J., Smith, C. A., Thoden, J. B., Smith, R., Sutoh, K., Holden, H. M. & Rayment, I. (1995). *Biochemistry*, **34**, 8960–8972.

Geeves, M. A. & Conibear, P. B. (1995). *Biophys. J.* **68**, Suppl. 4, 199S–201S.

Gulick, A. M., Bauer, C. B., Thoden, J. B. & Rayment, I. (1997). *Biochemistry*, **36**, 11619–11628.

Holmes, K. C. (1997). *Curr. Biol.* **7**(2), R112-R118.

Holmes, K. C., Popp, D., Gebhard, W. & Kabsch, W. (1990). *Nature (London)*, **347**, 44–49.

Houdusse, A. & Cohen, C. (1996). *Structure*, **4**(1), 21–32.

Huston, E. E., Grammer, J. C. & Yount, R. G. (1988). *Biochemistry*, **27**, 8945–8952.

Huxley, A. F. & Niedergerke, R. M. (1954). *Nature (London)*, **173**, 971–973.

Huxley, H. E. (1952). PhD, Cambridge University, England.

Huxley, H. E. (1957). *Biophys. Biochem. Cytol.* **3**, 631–648.

Huxley, H. E. (1969). *Science*, **164**, 1356–1366.

Huxley, H. E. & Brown, W. (1967). *J. Mol. Biol.* **30**, 383–434.

Huxley, H. E. & Hanson, J. (1954). *Nature (London)*, **173**, 973–976.

Huxley, H. E., Simmons, R. M., Faruqi, A. R., Kress, M., Bordas, J. & Koch, M. H. J. (1981). *Proc. Natl Acad. Sci. USA*, **78**, 2297–2301.

Irving, M., Lombardi, V., Piazzesi, G. & Ferenczi, M. A. (1992). *Nature (London)*, **357**, 156–158.

Irving, M., St Claire Allen, T., Sabido-David, C., Craik, J. S., Brandmeier, B., Kendrick-Jones, J., Corrie, J. E., Trentham, D. R. & Goldman, Y. E. (1995). *Nature (London)*, **375**, 688–691.

Jontes, J. D., Wilson-Kubalek, E. M. & Milligan, R. A. (1995). *Nature (London)*, **378**, 751–753.

Kabsch, W. & Holmes, K. C. (1995). *Faseb J.* **9**(2), 167–174.

Kabsch, W., Mannherz, H. G., Suck, D., Pai, E. F. & Holmes, K. C. (1990). *Nature (London)*, **347**, 37–44.

Kraulis, P. J. (1991). *J. Appl. Cryst.* **24**, 946–950.

Kurzawa, S. E., Manstein, D. J. & Geeves, M. A. (1997). *Biochemistry*, **36**, 317–323.

Lorenz, M., Popp, D. & Holmes, K. C. (1993). *J. Mol. Biol.* **234**, 826–836.

Lymn, R. W. & Taylor, E. W. (1971). *Biochemistry*, **10**, 4617–4624.

Margossian, S. S. & Lowey, S. (1973a). *J. Mol. Biol.* **74**, 301–311.

Margossian, S. S. & Lowey, S. (1973b). *J. Mol. Biol.* **74**, 313–330.

Merritt, E. A. & Bacon, D. J. (1997). *Methods Enzymol.* **277**, 505–524.

Mornet, D., Pantel, P., Audemard, E. & Kassab, R. (1979). *Biochem. Biophys. Res. Commun.* **89**, 925–932.

Nicholls, A., Sharp, K. A. & Honig, B. (1991). *Proteins*, **11**, 281–296.

Rayment, I., Holden, H. M., Whittaker, M., Yohn, C. B., Lorenz, M., Holmes, K. C. & Milligan, R. A. (1993). *Science*, **261**, 58–65.

Rayment, I., Rypniewski, W. R., Schmidt-Base, K., Smith, R., Tomchick, D. R., Benning, M. M., Winkelmann, D. A., Wesenberg, G. & Holden, H. M. (1993). *Science*, **261**, 50–58.

Reedy, M. K., Holmes, K. C. & Tregear, R. T. (1965). *Nature (London)*, **207**, 1276–1280.

Rosenbaum, G., Holmes, K. C. & Witz, J. (1971). *Nature (London)*, **230**, 434–437.

Schlichting, I., Becker, A., Manstein, D. & Holmes, K. C. (1998). In preparation.

Schroeder, R., Angert, I., Jahn, W. & Holmes, K. C. (1998). In preparation.

Schroeder, R. R., Manstein, D. J., Jahn, W., Holden, H., Rayment, I., Holmes, K. C. & Spudich, J. A. (1993). *Nature (London)*, **364**, 171–174.

Smith, C. A. & Rayment, I. (1996a). *Biochemistry*, **35**, 5404–5417.

Smith, C. A. & Rayment, I. (1996b). *Biophys. J.* **70**, 1590–1602.

Uyeda, T., Abramson, P. D. & Spudich, J. A. (1996). *Proc. Natl Acad. Sci. USA*, **93**, 4459–4464.

Whittaker, M., Wilson-Kubalek, E. M., Smith, J. E., Faust, L., Milligan, R. A. & Sweeney, H. L. (1995). *Nature (London)*, **378**, 748–751.

Yount, R. G., Lawson, D. & Rayment, I. (1995). *Biophys. J.* **68**, Suppl. 4, 47S–49S.